Self-Assembly of Rigid and Coil Polymers into Hollow Spheres in Their Common Solvent

Hongwei Duan, Min Kuang, Jing Wang, Daoyong Chen, and Ming Jiang*

Department of Macromolecular Science and The Key Laboratory of Molecular Engineering of Polymers, Fudan University, Shanghai, 200433, China

Received: August 6, 2003; In Final Form: November 6, 2003

This paper studies self-assembly of a rigid oligomer, polyimide (PI) with carboxyl ends, and a proton-accepting polymer poly(4-vinylpyridine) (PVPy) or poly(styrene-*co*-4-vinylpyridine) (SVP) in solutions. It was found that these rigid/coil polymer pairs could form submicrometer hollow spheres in their common solvent chloroform. The rigid character of PI and its hydrogen-bonding grafting to PVPy chains are the key factors for such unique self-assembly behavior. Over a broad composition range, decreasing the ratio of PI/PVPy was found unfavorable to the assembly, i.e., leading to larger and broadly distributed hollow spheres. As the weight ratio of PI/PVPy decreased to 0.5 or less, the hollow spheres disappeared and soluble complex formed. PI could form hollow spheres with SVP as well, provided the pyridine unit content in SVP was not less than 11 mol %. With regard to the effect on the aggregate size and its distribution, decreasing the pyridine content in SVP was found equivalent to decreasing the PI/PVPy ratio. The structure of the hollow spheres of PI/SVP could be locked by chemical cross-linking SVP, and TEM studies showed that the cross-linked particles were able to maintain their integrity. Scanning electron micrographs of the solvent-cast films of the hollow-sphere solutions showed a two-dimensional hexagonal close-packing lattice of circular holes in a polymer matrix, similar to that for rod−coil block copolymers reported in the literature. Our work proved that this regular pattern was induced by water droplets and their packing in the process of dewetting of the polymer solutions.

Introduction

Self-assembly of polymers leading to nanostructures with novel morphologies and properties has been an active area in the past decade.[1−3] Among the variety of targeting materials, hollow spheres on nanometer and submicrometer scales have attracted much attention owing to their potentials for serving as carriers of catalysts, enzymes, drugs, etc.[4] Self-assembly of block copolymers[5−8] and template approaches[9−11] are both proven to be effective ways to obtain these functional materials.

Recently, our research efforts have been devoted to developing a block-copolymer-free strategy to fabricate micelles based on homopolymer pairs. This novel approach results in noncovalently connected micelles (NCCM), in which only hydrogen bonds rather than chemical bonds exist between the shell and core.[12] As a typical example, the NCCM composed of poly(4-vinylpyridine) (PVPy) shell and hydroxyl-containing polystyrene (PS(OH)) core was realized in a selective solvent for PVPy due to hydrogen bonding between the hydroxyl groups and pyridine units. Furthermore, subsequent cross-linking of the PVPy shell and dissolution of the PS(OH) core moiety led to hollow spheres.[12c]

When we used a rigid oligomer, polyimide (PI) with carboxyl ends, as a building block to fabricate NCCM with PVPy in their common solvent, chloroform, hollow spheres were unexpectedly obtained.[12e] Comparing with the existing procedures for producing micelles and hollow spheres, this process of using rigid−coil homopolymer pairs in their common solvent seemed much simpler and more straightforward. As we demonstrated previously, this unusual phenomenon can be attributed to two main factors: the rigid character of PI and its "grafting" to the PVPy chains. In fact, it was reported that self-assembly of rod−coil block copolymers resulted in some unprecedented morphologies both in their selective solvents[8] and in the solid state.[2a] The propensity to parallel packing of the rod blocks was believed to play an important role in such unusual assembly behavior. This work aims at a further understanding of the self-assembly of the rigid−coil homopolymer pairs in their common solvent, particularly, its dependence on some factors such as weight ratio of the two polymers, the content of proton-acceptor sites, and the molecular weight of the main chains. In addition, the pattern formation in cast film of the hollow aggregates is studied.

Experimental Section

Sample Preparation. The PI (Scheme 1) with two carboxyl ends was synthesized by condensation polymerization of bisphenol A dianhydride and 3,3′-dimethylbenzidine and then capped with trimellitic anhydride (Scheme 1) in dimethylacetamide at room temperature followed by chemical imidization with acetic anhydride and triethylamine and thermoimidization up to 200 °C. The molecular weights were determined by size exclusion chromatography using THF as eluent based on polystyrene calibration. Its number- and weight-average molecular weights were 4600 and 9280, respectively. The glass transition temperature (T_g) was as high as 233 °C, reflecting the stiffness of the chains. Samples of poly(4-vinylpyridine) (PVPy) were synthesized and purified as described elsewhere.[13] The viscosity-average molecular weight M_η of PVPy1 and PVPy2 are 1.4×10^5 and 8.0×10^4, and accordingly the numbers of the repeating unit are 1330 and 760, respectively. The copolymers SVP*n* (*n* indicates the molar fraction of 4-vinylpyridine) were synthesized by free radical copolymerization of styrene and vinylpyridine, and the characterization data are listed in Table 1.

* Corresponding author. E-mail: mjiang@fudan.edu.cn.

10.1021/jp0363139 CCC: $27.50
Published on Web 12/16/2003

SCHEME 1: Chemical Structures of Polyimide (PI), Trimellitic Anhydride, and Poly(amic acid ester) PAE

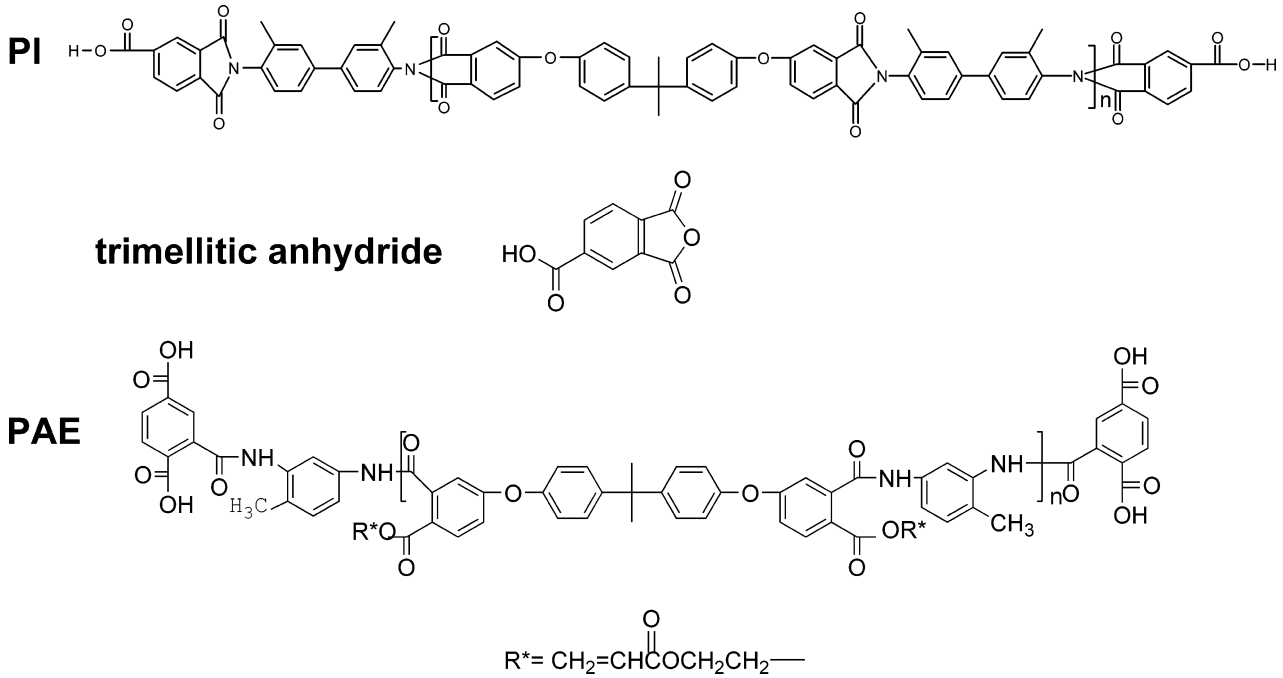

TABLE 1: Characterization Data of SVP*n* Copolymers

SVP*n* copolymers	4-vinylpyridine content, %	$M_w \times 10^{-4}$,[a] g/mol	T_g, °C
SVP32	32.29	5.19	121
SVP16	16.18	2.94	114
SVP11	11.02	2.67	112
SVP7	6.66	2.54	110

[a] M_w was determined by size exclusion chromatography using DMF as eluent based on polystyrene calibration.

Preparation of Hollow Aggregates. A desired amount of PI dilute solution in chloroform was added dropwise to PVPy (SVP*n*) solution in chloroform under ultrasonic conditions. Except for the case of studying the influence of dilution, in the final solution the concentration of PVPy (SVP*n*) was 0.10 mg/mL and the concentration of PI depended on the required ratio of PI/PVPy (SVP*n*). With the addition of PI solution in chloroform, the solution turned to slightly bluish, which indicated the formation of aggregates of PI/PVPy (SVP*n*).

Dynamic Light Scattering (DLS). A commercial LLS spectrometer (ALV/SP-125) equipped with an ALV-5000 multi-τ digital time correlator and a solid-state laser (DPPS, output power = 400 mW, at λ = 532 nm) was used. All the measurements were done at 25.0 ± 0.1 °C. In DLS, the Laplace inversion of intensity−intensity−time correlation function $G^{(2)}(t,q)$ can result in the line width distribution $G(\Gamma)$. Furthermore, $G(\Gamma)$ can be converted into a transitional diffusion coefficient distribution $G(D)$ or a hydrodynamic radius distribution $f(R_h)$ via the Stokes−Einstein equation, $\langle R_h \rangle = k_B T/6\pi\eta D$, where η, k_B, and T are the solvent viscosity, the Boltzmann constant, and the absolute temperature, respectively. In all cases, the time correlation functions were measured at a scattering angle 30°.

Transmission Electron Microscopy. TEM observations were performed on a Philips CM120 electron microscope at an accelerating voltage of 80 kV. In the preparation of the specimen for observing the discrete aggregates, 5 μL of the aggregate solution was dropped on a carbon-coated copper grid, which was frozen in liquid N_2 just before being used, followed by solvent evaporation at room temperature.

Scanning Electron Microscopy. SEM observations were performed on a Philips XL30 electron microscope at an accelerating voltage of 20 or 25 kV. For the sample preparation, a carbon-coated grid was dipped quickly into the micellar solution and then was dried in a flow hood at room temperature. The specimens were coated with gold before SEM observations.

Results and Discussion

Self-Assembly of PI and PVPy into Hollow Spheres. In our previous communication,[12e] we reported that mixing PI and PVPy in their common solvent $CHCl_3$ led to submicron hollow spheres with PI as the inner shell and PVPy as the outer shell. Our recent study on self-assembly of a cross-linkable rigid polymer, e.g., photosensitive carboxyl-terminated poly(amic acid) ester (PAE, Scheme 1) and PVPy in THF also led to hollow aggregates with an outer PVPy shell and an inner PAE shell.[14] The key factors affecting the self-assembly of these two polymer pairs are believed to be the hydrogen bonding between the carboxyl end groups of PI (or PAE) and pyridine units of PVPy and the requirement of effective packing of the "grafted" rigid PI (or PAE) rods. Herein, we studied this self-assembly behavior of PI and PVPy in chloroform over a broad composition of PI/PVPy1 (w/w) ranging from 17 to 0.2 and accordingly the chain number ratio of PI to PVPy1 between 517 and 6.0. The dynamic light scattering results for the blend solutions of PI/PVPy1 with weight ratio from 17 to 3 are shown in Figure 1, which clearly demonstrates the formation of submicron-sized aggregates. The detailed data are listed in Table 2.

Although both PVPy and PI are polydispersed homopolymers and there are no chemical bonds between them, the aggregates displayed narrow size distributions as indicated by the small polydispersity index (PDI). Figure 2 shows the hydrodynamic radius of PI/PVPy as a function of the blend composition. Two systems of PI/PVPy1and PI/PVPy2 show the same variation trend: i.e., over the composition range, $\langle R_h \rangle$ apparently increases with the decreasing ratio of PI/PVPy ranging from 17.0 to 3.0.

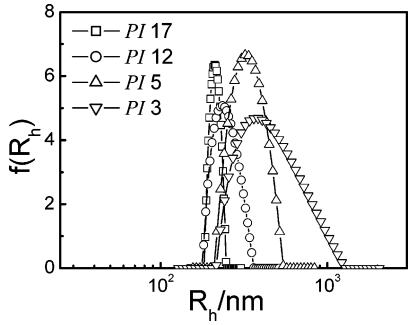

Figure 1. Hydrodynamic radius distribution of PI/PVPy1 hollow aggregates in chloroform with different PI/PVPy1 weight ratios measured by DLS (PI *n*; *n* is the weight ratio of PI/PVPy1). C_{PVPy} = 0.1 mg/mL.

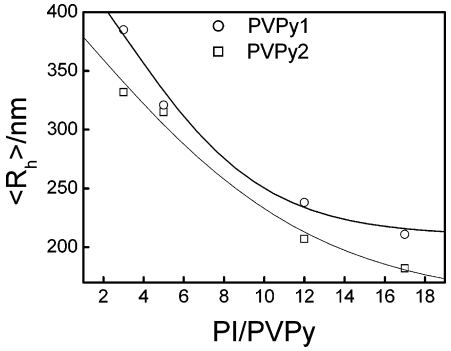

Figure 2. $\langle R_h \rangle$ of PI/PVPy hollow aggregates versus weight ratio of PI to PVPy. C_{PVPy} = 0.1 mg/mL.

TABLE 2: Characterization Data of the Hollow Spheres of PI/PVPy1 (M_η= 140 000) and PI/PVPy2 (M_η = 80 000) Measured by DLS; C_{PVPy} = 0.1 g/mL

	PVPy1		PVPy2	
PI/PVPy (w/w)	$\langle R_h \rangle$, nm	PDI	$\langle R_h \rangle$, nm	PDI
17	211	0.01	182	0.06
12	238	0.02	207	0.04
5	321	0.04	315	0.02
3	385	0.11	332	0.04
1	10/507			
0.5			11/250	
0.2	21	0.27	24	0.25

This means that more grafts favor the formation of small aggregates. As discussed in our previous papers, it is the propensity to parallel packing of the PI grafts that results in the hollow spheres. Obviously, the larger the value of PI/PVPy is, the larger the "grafted density" of PI along the PVPy chains is. Consequently, such dense grafts promote the fine dispersion.

This trend of the aggregate size varying with the "graft density" is similar to that reported for the micelles of graft copolymers and hydrogen bonding graft copolymers in selective solvents, although the mechanism for the aggregate formation is different. For example, the size of the micelles of graft copolymer PAA-*graft*-PS with PS core decreased with increasing graft density.[15] For NCCM of carboxyl-ended polybutadiene (CPB) and PVPy with CPB core, Wang et al. found a similar dependence of NCCM on the weight ratio of CPB/PVPy.[12b] A reasonable inference of this finding for PI/PVPy is that there must be a minimum value of the ratio of PI to PVPy for the formation of the aggregates.

In fact, we found that as the weight ratio of PI/PVPy1 decreased to 1.0, a bimodal distribution of $\langle R_h \rangle$ of the solution was observed (Figure 3). The peak located at 507 nm was related to the large aggregates, and that at 10 nm could be attributed to

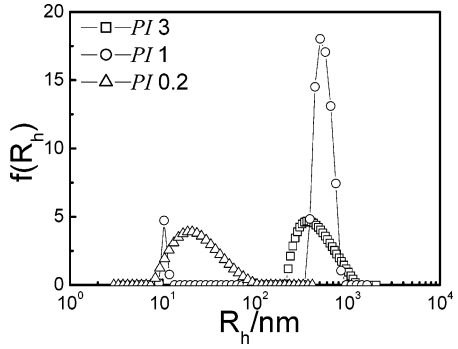

Figure 3. Hydrodynamic radius distribution of PI/PVPy1 aggregates in chloroform with different PI/PVPy1 weight ratios measured by DLS (PI *n*; *n* is the weight ratio of PI/PVPy1). C_{PVPy1} = 0.1 mg/mL.

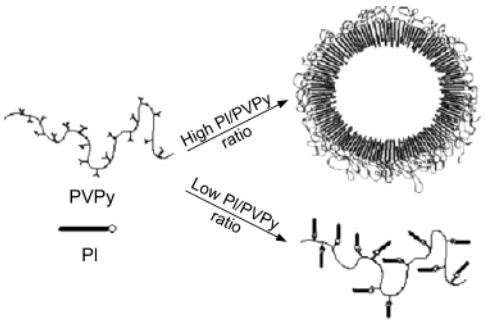

Figure 4. Schematic illustration of the formation of the hollow spheres and soluble complex.

individual PVPy1 molecules as this value is almost the same as that found for pure PVPy1 solutions in chloroform, $\langle R_h \rangle \sim$ 11 nm. In this PI/PVPy1 ratio, even all the rigid PI chains in the solutions were attached to PVPy, with only 30 PI grafts for each PVPy1 chain containing about 1330 pyridine units. This small portion of the grafts was not enough to make all PVPy chains form large aggregates. Finally, as the PI/PVPy1 ratio decreased further to 0.2, i.e., each PVPy chain might carry six grafts of PI, only a peak located at around 21 nm was observed which could be attributed to the soluble graft copolymer of PI and PVPy1. Similarly, in NCCM of CPB and PVPy with CPB core, there were also individual grafted PVPy chains existing in the solution when every PVPy chain carried only one CPB graft on average.[12b] This observation for PI/PVPy1 indicates a transition from hollow aggregates to complex as the ratio of PI to PVPy declines to a certain value.

Table 2 also shows the results for PI/PVPy2, in which the molecular weight of PVPy2 is apparently smaller than that of PVPy1. The hollow spheres were formed when the weight ratio varied from 17.0 to 3.0. It can be found that at the same weight ratio of PI/PVPy, $\langle R_h \rangle$ of the hollow aggregates from PVPy2 and PI was evidently smaller than that of PVPy1 and PI. Furthermore, the transition from hollow spheres to soluble complex was observed in PI/PVPy2 as well. The aggregates and single molecules coexisted as the ratio of PI/PVPy2 decreased to 0.5, and finally the aggregates disappeared as the ratio decreased further to 0.2. Thus the aggregation behavior of PI/PVPy at different compositions can be illustrated schematically in Figure 4. This illustration displays the difference between a hollow sphere and interpolymer complex. However, at the moment, we are still not able to give details of the structure of the hollow spheres; e.g., due to the presence of carboxyl groups at both ends of PI, the three-layer structure of PVPy−PI−PVPy cannot be excluded.

Figure 5 shows that the size of the aggregates of PI/PVPy1 significantly increased with dilution of the solution. This

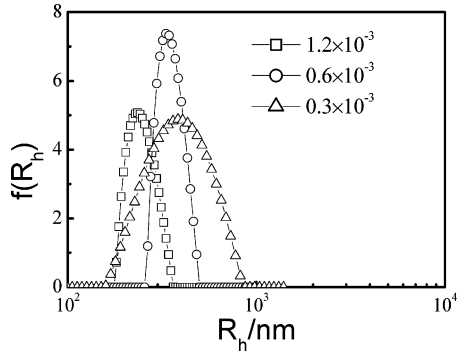

Figure 5. Swelling of hollow spheres of PI/PVPy1 (w/w, 12/1) measured by DLS.

TABLE 3: Characterization Data of the Hollow Spheres of PI/SVP*n* Measured by DLS; C_{SVPn} = 0.1 mg/ML

SVP*n* copolymers	PI/SVP*n* (w/w)	$\langle R_h \rangle$ (nm)	PDI
SVP32	10	216	0.03
SVP32	7.5	259	0.07
SVP32	5	280	0.04
SVP16	10	340	0.06
SVP11	10	345	0.11

behavior is completely different from that found for ordinary polymeric micelles. For example, Zhang et al.[16] reported that the structure of the crew-cut micelle of PS-*b*-PAA was frozen below the glass transition temperature of the polystyrene block, so that the aggregation number was not influenced by dilution. The same phenomenon was also found in surfactant-free dispersed polymer particles.[17,18] In the present cases, both PI and PVPy are in their good solvent, and the formation of the aggregates is associated with the high local chain density of PI surrounding the PVPy chains. Decreasing the total concentration of the component polymers is unfavorable to the "grafting", and consequently, the equilibrium may shift to less "graft density" which leads to larger spheres with higher aggregation number.

Self-Assembly of PI and SVP*n* Copolymers. The results shown above indicate an apparent dependence of self-assembly of PI and PVPy on the "graft density" of PI to PVPy. To further understand this rule, PVPy was replaced by SVP*n* copolymers, in which the interaction sites (pyridine) and inert polystyrene units are randomly distributed. The DLS data in Table 3 show that the copolymers with respective pyridine unit fractions of 11, 16, and 32% could also form hollow aggregates in chloroform. The size of the aggregates increases when the content of 4-vinylpyridine in the copolymers decreases. Meanwhile, the aggregates display a much broader distribution when the pyridine content decreases to 11%. Furthermore, no aggregates in the solution were detected by DLS when the content of 4-vinylpyridine declined to 7%. However, for SVP7, aggregates were observed in a selective solvent for PVPy, i.e., chloroform/cyclohexane (v/v, 2/8). In short, there is a minimum value of the relative amount of the proton-accepting groups along the chain for forming hollow spheres. Similar with PI/PVPy, PI/SVP32 also shows an apparent dependence of the aggregation on the composition; e.g., the size decreased with increasing ratio of PI/SVP32 (Table 3).

All the results confirmed the argument that the propensity to parallel packing of the rigid PI grafts is the main driving force for the aggregation. Decreasing the pyridine content in SVP is obviously unfavorable to the formation of the aggregation, i.e., leading to large and broadly distributed spheres. The work

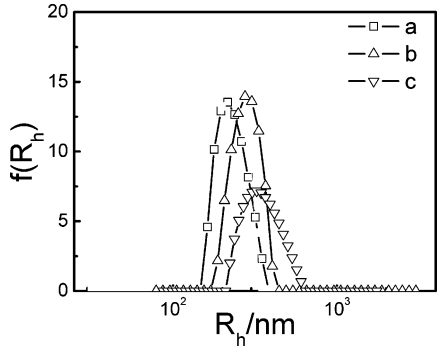

Figure 6. Hydrodynamic radius distribution of PI/SVP32 (w/w, 10/1) hollow aggregates in chloroform and cross-linked ones measured by DLS at 25 ± 0.1 °C. a, hollow spheres in chloroform; b, cross-linked hollow spheres in chloroform; c, cross-linked hollow spheres in chloroform/DMF (v/v, 1/1).

proved that, with regard to the self-assembly, decreasing the PI/PVPy ratio is equivalent to decreasing the pyridine content in SVP.

Stabilization of the Hollow Spheres. Because the noncovalent bond, e.g., hydrogen bonding, is responsible for the formation of hollow aggregates, their structures are sensitive to solvent and temperature changing. To produce hollow spheres with a robust structure, we tried to use 1,4-dibromobutane as a cross-linker for PVPy.[19] Thus, 100 mol % 1,4-dibromobutane based on the pyridine units in the hollow spheres of SVP-32 and PI was added, and the mixture was kept at 45 °C for 2 days. In a control experiment, the hollow sphere solution without the cross-linker was treated at the same condition. As shown in Figure 6, after the reaction, the cross-linked hollow spheres displayed a lager radius of 275 nm compared with 216 nm for the precursors. Furthermore, after addition of an equivolume of dimethyformamide (DMF) in the solution, which could lead to dissociation of hydrogen bonding, the cross-linked hollow spheres displayed a size expansion up to 324 nm, while for the control experiment, aggregates disappeared as indicated by DLS. This means that the structure of hollow spheres of SVP32−PI was successfully locked in by the cross-linking.

It was interesting to find that the structure of the hollow spheres composed of PI and homopolymer PVPy could not be locked by cross-linking at the same condition as the reaction led to macroscopic precipitate in the solution. On the basis of the bilayered structure of the hollow aggregates, we suggested it could be assumed that the soluble polystyrene units of the copolymers SVP probably enriched in the most outer part of the shell of the hollow spheres, which could obviously prevent interparticle cross-linking. However, for the case of homopolymer PVPy without such shielding of the PS segments, interparticle cross-linking occurred and led to macroscopic precipitation.

Morphologies of the Hollow Spheres and Cross-linked Spheres. Figure 7a shows a TEM micrograph of PI/PVPy32 (12/1, w/w). The morphology of the particles explored by TEM here is very similar to that of the aggregates of PI/PVPy reported previously.[12e] There are two main feathers of the morphology of the aggregates. First, the obvious contrast between the central part and outer part can be attributed to the hollow structure of the aggregates, as reported for different kinds of particles with a central cavity.[7,8,12b,12e] Second, there is a large deformation of the particles leading to an irregular outline. This deformation is believed to occur during the process of the solvent evaporation in the sample preparation, as there is no chemical bonding between the inner and outer shells causing instability of the

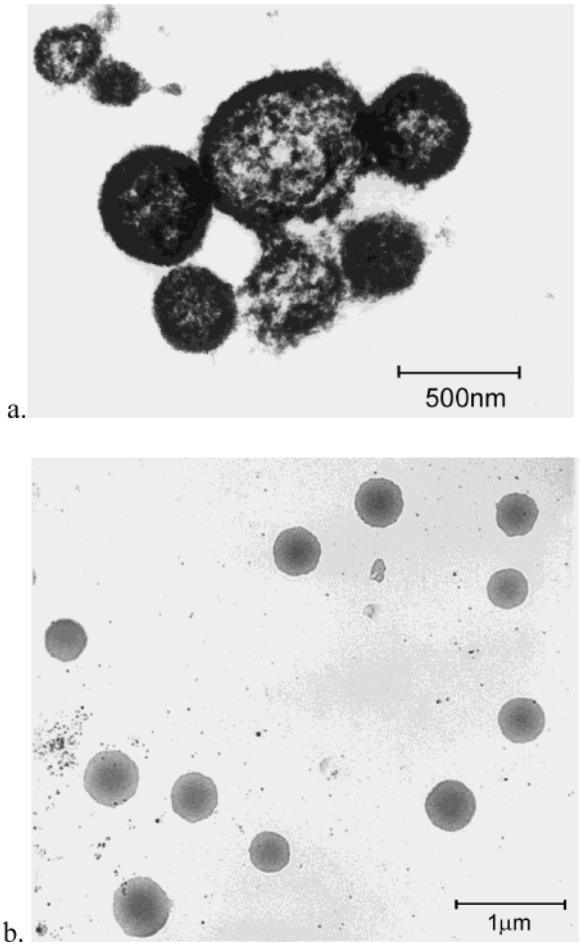

Figure 7. TEM micrographs of hollow spheres of PI/SVP32 (w/w, 10:1) (a) and corresponding cross-linked spheres (b).

sample shape. As proved by DLS studies, cross-linking the outer shell of PVPy of the aggregate successfully locked the structure. This conclusion is confirmed by our TEM (Figure 7b) for the cross-linked aggregates of PI/SVP-32. The particles shown in Figure 7b possess regular spherical shape, indicating that the cross-linked particles are able to persist their integrity during the solvent evaporation and at high vacuum. In Figure 7b, although we can see a thin and dark outline of the spheres, no bright domains can be found within the spheres. Considering all these facts, we suppose that, after cross-linking the outer shell of PVPy, it could be possible that the PI chains as rods did not penetrate readily through the PVPy network and thus remained within the sphere. In addition, the resultant quaternary pyridine groups in the cross-linking reaction no longer interact with PI; therefore, PI chains may distribute homogeneously within the aggregates rather than form an inner shell. This argument can explain the TEM observations. This result was obviously different from NCCM of PVPy and modified polystyrene, PS(OH).[12c] In that case, the DLS and TEM results proved that cavitation of the assembled spheres occurred due to the removal of the flexible PS(OH) chains from the spheres when DMF was added. This difference between the cross-linked spheres of PI/PVPy and those of PS(OH)/PVPy in the DMF-dominated solvents may indicate that the rigid PI is much more difficult to penetrate through the PVPy network from the interior of the micelle into the solution than the coil-like PS(OH) chains do.

Formation of Two-Dimensional Microporous Structure in Solvent-Cast Film. The solvent-cast film of the aggregates (PI/PVPy1 = 12:1, w/w) on copper grids prepared in a flow

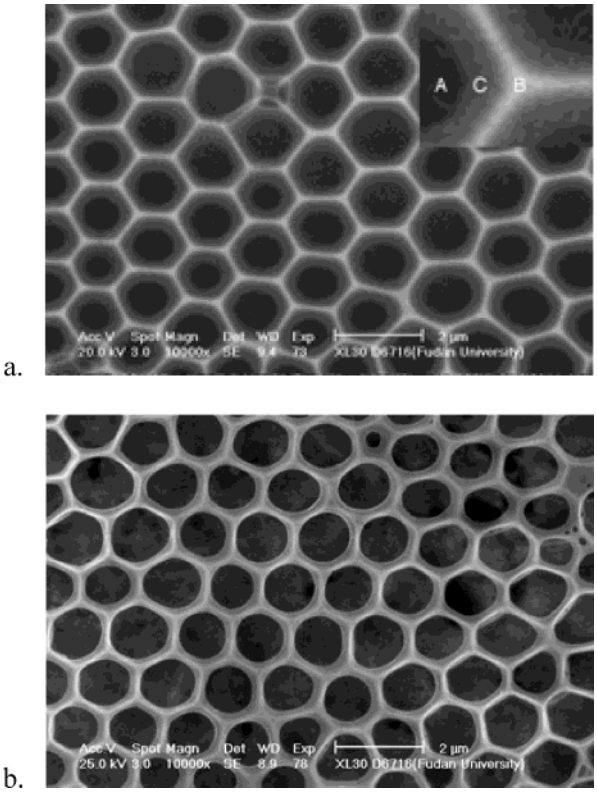

Figure 8. SEM micrographs of solvent-cast film of hollow-sphere solutions: PI/PVPy1 (w/w, 12/1) (a), at high magnification (insert), and PI/SVP32 (w/w, 10:1) (b).

hood showed a feature containing a two-dimensional hexagonal close-packing lattice of circular holes in a polymer matrix found by SEM observations (Figure 8a). Each building unit here contains a prominent hexagonal framework and a central hole with a diameter of approximately 1 μm. The details of the polymeric backbone are shown in the inset of Figure 8a. Using energy-dispersive X-ray microanalysis (PV971053, Phoenix) attached to the TEM for selective areas with a diameter of 30 nm, a rough estimation of the compositions in typical microareas was made. No nitrogen was detected at point A, indicating that it was a void area. The signal intensity ratio of nitrogen to oxygen at point B was about double that at point C. As the nitrogen content in PVPy is much higher than that in PI and only PI contains oxygen, the microanalysis results imply that the central backbone and the two sides are respectively rich in PVPy and PI. In addition, in the case of SVP32 and PI, microporous films also were produced (Figure 8b).

This observed feature of the hexagonal submicroporous pattern is quite similar to that reported for the cast film of rod−coil block copolymers in selective solvent by Jenekhe et al.[8b] The authors attributed this to a regular packing of the hollow spheres on the substrate.

We noticed that, in recent years, such regular hexagonal microporous structure has been reported by several research groups in the literature.[20−23] This structure could be prepared from a variety of polymers and surfactants. François et al. first found that hexagonal microporous film was produced during casting CS_2 solution of rod−coil polystyrene-*b*-poly(*p*-phenylene) under humid conditions.[20] Hadziioannou et al.[21] also obtained microporous film from rod−coil block copolymer polystyrene-*b*-poly(2,5-dioctyloxy-*p*-phenylenevinylene) in the same way. The family of source materials to form these honeycomb-like films in this approach was extended greatly by Shimomura and co-workers.[22] They found polystyrene-*b*-

polyisoprene block copolymer, amphiphilic polyion complex (e.g., DNA and amphiphile complex), and organic−inorganic hybrids also could form the hexagonal microporous structure in the cast films. As reported in the work, the prerequisites of the formation of the microporous films are a water-immiscible solvent being used and a certain humidity in sample preparation. It was found that the hexagonal pattern actually originated from the presence of water droplets and their regular packing in the process of dewetting of the polymer solutions. To know whether this mechanism is applicable to the present case, solvent casting of our hollow spheres of PI and PVPy in chloroform was carried out in a drying box. SEM results showed that there was no longer any microporous film formed in the resultant film. This evidence clearly supported the mechanism of water droplet induced pattern.

Besides, we found that the composition of hollow spheres had an influence on the frame thickness between the pores and pore diameter. The results showed that lowering the weight ratio of PI/PVPy at a constant concentration of PVPy and accordingly the total concentration caused a thinner frame and lager pore diameter (data not shown). In the work of Shimomura,[22] similar results also were obtained; i.e., the higher concentrations led to smaller pores and thicker walls.

Acknowledgment. This work is financially supported by NNSFC (Nos. 50333010, 50173006); part of the light scattering measurements was performed at Prof. Wu's laboratory, Chinese University of Science and Technology, Hefei, China; the PI sample was kindly supported by Miss W. J. Gan and Prof. S. J. Li, Fudan University.

References and Notes

(1) Muthukumar, M.; Ober, C. K.; Thomas, E. L. *Science* **1997**, *277*, 1225.

(2) (a) Stupp, S. I.; LeBonheur, V.; Walker, K.; Li, L. S.; Huggins, K. E.; Keser, M.; Amstutz, A. *Science* **1997**, *276*, 384. (b) Klok, H. A.; Lecommandoux, S. *Adv. Mater.* **2001**, *13*, 1217.

(3) Dennis, E. D.; Eisenberg, A. *Science* **2002**, *297*, 967.

(4) (a) Bergbreiter, D. E. *Angew. Chem., Int. Ed.* **1999**, *38*, 2870. (b) Meier, W. *Chem. Soc. Rev.* **2000**, *29*, 295.

(5) (a) Huang, H. Y.; Remsen, E. E.; Kowalewski, T.; Wooley, K. L. *J. Am. Chem. Soc.* **1999**, *121*, 3805. (b) Zhang, Q.; Remsen, E. E.; Kowalewski, T.; Wooley, K. L. *J. Am. Chem. Soc.* **2000**, *122*, 3642.

(6) (a) Stewart, S.; Liu, G. J. *Chem. Mater.* **1999**, *11*, 1048. (b) Ding, J. F.; Liu, G. J. *J. Phys. Chem. B* **1998**, *282*, 1111.

(7) Sanji, T.; Nakatsuka, Y.; Ohishi, S.; Sakurai, H. *Macromolecules* **2000**, *33*, 8524.

(8) (a) Jenekhe, S. A.; Chen, X. L. *Science* **1998**, *279*, 1903. (b) Jenekhe, S. A.; Chen, X. L. *Science* **1999**, *283*, 372.

(9) Caruso, F.; Caruso, R. A.; Möhwald, H. *Science* **1998**, *282*, 1111.

(10) Donath, E.; Sukhorukov, G. B.; Caruso, F.; Davis, S. A.; Möhwald, H. *Angew. Chem., Int. Ed.* **1998**, *37*, 2202.

(11) (a) Hotz, J.; Meier, W. *Langmuir* **1998**, *14*, 1031. (b) Sauer, M.; Meier, W. *Chem. Commun.* **2001**, 55.

(12) (a) Yuan, X. F.; Jiang, M.; Zhao, H. Y.; Wang, M.; Wu, C. *Langmuir* **2001**, *17*, 6122. (b) Wang, M.; Zhang, G. Z.; Chen, D. Y.; Jiang, M.; Liu, S. Y. *Macromolecules* **2001**, 34, 7172. (c) Wang, M.; Jiang, M.; Ning, F. L.; Chen, D. Y.; Liu, S. Y.; Duan, H. W. *Macromolecules* **2002**, *35*, 5980. (d) Liu, X. Y.; Jiang, M.; Yang, S. L.; Chen, M. Q.; Chen, D. Y.; Yang, C.; Wu, K. *Angew. Chem., Int. Ed.* **2002**, *41*, 2950. (e) Duan, H. W.; Chen, D. Y.; Jiang, M.; Gan, W. J.; Li, S. J.; Wang, M.; Gong, J. *J. Am. Chem. Soc.* **2001**, *123*, 12097.

(13) Liu, S. Y.; Zhang, G. Z.; Jiang, M. *Polymer* **1999**, *40*, 5449.

(14) Kuang, M.; Duan, H. W.; Wang, J.; Chen, D. Y.; Jiang, M. *Chem. Commun.* **2003**, 496.

(15) Ma, Y. H.; Cao, T.; Webber, S. E. *Macromolecules* **1998**, *31*, 1773.

(16) Zhang, L. F.; Barlow, R. J.; Eisenberg, A. *Macromolecules* **1995**, *28*, 6055.

(17) Li, M.; Zhang, Y. B.; Jiang, M.; Zhu, L.; Wu, C. *Macromolecules* **1998**, *31*, 6841.

(18) Liu, S. Y.; Hu, T. J.; Liang, H. J.; Jiang, M.; Wu, C. *Macromolecules* **2000**, *33*, 8640.

(19) Frechet, J. M. J.; Meftahi, M. V. D. *Br. Polym. J.* **1984**, *16*, 193.

(20) Widawski, G.; Rawiso, B.; François, B. *Nature* **1994**, *369*, 387.

(21) de Boer, B.; Stalmach, U.; Nijland, H.; Hadziioannou, G. *Adv. Mater.* **2000**, *12*, 1581.

(22) (a) Karthaus, O.; Maruyama, N.; Cieren, X.; Shimomura, M.; Hasegawa, H.; Hashimoto, T. *Langmuir* **2000**, *16*, 6071. (b) Maruyama, N.; Koito, T.; Nishida, J.; Sawadaishi, T.; Cieren, X.; Ijiro, K.; Karthaus, O.; Shimomura, M. *Thin Solid Films* **1998**, *327−329*, 854.

(23) Stenzel-Rosenbaum, M. H.; Davis, T. P.; Fane, A. G.; Chen, V. *Angew. Chem., Int. Ed.* **2001**, *40*, 3428.